JOURNAL OF THERMOPHYSICS AND HEAT TRANSFER
Vol. 8, No. 1, Jan.–March 1994

Nonisothermal Turbulent Boundary-Layer Adverse Pressure Gradient Large Scale Thermal Structure Measurements

Nader Bagheri*
California Maritime Academy, Vallejo, California 94590
and
Bruce R. White† and Ting-Kwo Lei‡
University of California, Davis, Davis, California 95616

Hot-wire anemometry measurements in an incompressible turbulent boundary-layer flow over a heated flat plate under equilibrium adverse-pressure-gradient conditions ($\beta = 1.8$) were made for two different temperature difference cases (10 and 15°C) between the wall and the freestream. Space-time correlations of temperature fluctuations (T') were obtained with a pair of subminiature temperature fluctuation probes. The mean convection velocities, the mean inclination angles, and coherence characteristics of the T' large-scale structure were determined. The present temperature structures measurements for a nonisothermal boundary layer are compared to the zero-pressure-gradient case with identical temperature differences previously reported, in which the mean convection velocity of the T' structure was a function of position y^+ and independent of the limited temperature-difference cases tested. The three major findings of the present study, as compared to the zero-pressure-gradient case, are 1) the mean convection speed of the T' structure under $\beta = 1.8$ pressure-gradient conditions was found to be substantially lower in the logarithmic core region than the zero-pressure-gradient case. Additionally, the mean convection speed is felt by the authors to be a function of pressure-gradient parameter β; 2) the mean inclination angle of the T' structure to the wall under the adverse-pressure-gradient flow was 32 deg, which compares favorably to the 30-deg value of the zero-pressure-gradient case; and 3) the limited data suggests that the mean convection velocity of the T' structure is a function of y^+ and independent of the limited temperature-difference cases tested.

Nomenclature

dP/dx	=	longitudinal or streamwise pressure gradient
P	=	static pressure
Re_θ	=	Reynolds number, $u_\infty\theta/\nu$
$R_{T,T}$	=	cross-correlation coefficient
T	=	temperature
t	=	time
U	=	time-mean average streamwise velocity
u	=	instantaneous streamwise velocity
u^*	=	friction velocity
v	=	instantaneous normal velocity
x	=	streamwise direction
y	=	normal direction
z	=	spanwise direction
β	=	pressure coefficient parameter, $(\delta^*/\tau_w)(dP/dx)$
Δ	=	Clauser boundary-layer thickness
δ	=	hydrodynamic boundary-layer thickness
δ_t	=	thermal boundary-layer thickness
δ^*	=	displacement boundary-layer thickness
θ	=	momentum-deficit thickness
ν	=	kinematic viscosity
τ_w	=	wall shear stress

Subscripts

∞	=	freestream
cv	=	convection velocity
f	=	reference
rms	=	root-mean-square value
w	=	wall

Superscripts

$'$	=	fluctuating quantity
$+$	=	normalization with viscous units, u^* and ν

Presented as Paper 92-0550 at the AIAA 30th Aerospace Sciences Meeting and Exhibit, Reno, NV, Jan. 6–9, 1992; received May 29, 1992; revision received Feb. 24, 1993; accepted for publication Feb. 25, 1993.

*Associate Professor, Department of Engineering. Member AIAA.
†Professor, Department of Mechanical Engineering. Member AIAA.
‡Graduate Student, Department of Mechanical Engineering. Student Member AIAA.

Introduction

THE space-time correlation measurements of velocity fluctuations for isothermal zero-pressure-gradient flows has been carried out by many investigators' measurements. Kline and Robinson[1] organized a community-wide survey and evaluation of coherent structures and motions in isothermal turbulent boundary layers. In their survey they defined the state of the turbulence structure knowledge.

Strataridakis et al.[2] obtained the space-time correlation of the u' and v' velocities and $u'v'$ using a pair of x-wire subminiature probes. They obtained the mean convection velocities, the mean inclination angles, and the spatial extent of the u', v', and $u'v'$ large-scale structures for a zero-pressure-gradient flow.

Information on the thermal and fluid structure of the flows with pressure-gradient effects is limited. Kline et al.[3] were one of the first to observe that a favorable pressure gradient reduced the rate of fluid bursting and, conversely, an adverse pressure gradient, increased the rate and intensity of bursting in the near wall region. From hot-wire measurements and combined dye and hydrogen bubble visualization, Kline et al.[3] also deduced that the average spanwise fluid streak spacing, when normalized with wall variables, is about 100 for all flows considered in their study, with or without the pressure gradients.

Lian[4] studied the fluid structure of the turbulent boundary layer under the condition of an adverse-pressure-gradient effect using flow visualization techniques. He observed that the

size of the coherent structures, especially in the vicinity of separation, were larger than the zero-pressure-gradient structure and, therefore, easier to observe and analyze.

The low- and high-speed streaks are universally observed in the wall region of turbulent boundary-layer flows. In zero-pressure-gradient flows, the low-speed fluid streaks are much narrower than the high-speed streaks.[3-5] However, in adverse-pressure-gradient boundary-layer flows, Lian[4] observed that the low-speed fluid streaks became almost as wide as high-speed streaks and, therefore, it is possible to observe the flow inside a low-speed streak.

The flow inside both low- and high-speed streaks is quiet and uniform, while the chaotic flow occurs along the interfaces of the low- and high-speed streaks.[4] The interface between low- and high-speed streaks, according to Lian, plays an important role in turbulence production.

An interesting feature of Lian's study was the observation of the generation of the so-called streamers. These streamers appeared to exist longer than the low- and high-speed streaks and were generated at the lateral edge between the low- and high-speed streaks. Reasons such as, why the long streamers exist, and why they resist longer than low- and high-speed streaks, are not clearly understood. However, Lian suggests that these long streams are believed to be the remains of the streamwise vortices and, thus, they can remain longer in the wall region.

Streamwise and transverse vortices were also observed in Lian's study. He observed that the streamwise vortices appeared to be stretching and forming downstream. The transverse vortices appeared at the front side of the high-speed streaks. The ends of the transverse vortices were linked to the lateral edges of the high-speed streaks.

White and Tiederman[6] studied the effect of pressure gradient and Reynolds number on the period of the burst cycle for a range of momentum thickness Reynolds number from 1120 to 2500. They considered a zero-pressure-gradient flow with two cases of mild and strong adverse pressure gradients. β in their study varied from 0 to 1.8. Over the range of Reynolds numbers considered, the results indicated that the burst period, when normalized with inner variables, was not a function of Reynolds number, but rather, exclusively a function of the pressure-gradient parameter. The period of the burst cycle was reduced as the magnitude of the pressure gradient was increased.

Little work has been reported in the literature regarding the thermal boundary-layer structure. The UC Davis research group were the first to show some results of thermal structure in a zero-pressure-gradient turbulent boundary-layer flow.[7] More recently, we reported the spatial characteristics of the zero-pressure-gradient thermal boundary-layer structure.[8]

In the present work, an extension of the earlier zero-pressure-gradient measurements is made. It involves the study of a turbulent boundary layer developing on a smooth heated surface in an adverse pressure gradient with an unheated starting length. Two temperature-difference cases between the wall and the freestream are investigated. The specific objective of the work is to obtain two-point correlations of the temperature fluctuation measurements from which calculations of mean convection velocities and mean inclination angles can be made for an adverse-pressure-gradient flow.

Experimental Facility

The experiments were carried out in an open-return-type wind tunnel with an overall length of 7.5 m. The entrance section has a 17-to-1 contraction ratio with a bell-mouth shape. Air filter, Hexcel honeycomb, and six screens are placed at the entrance of the converging section in order to remove the dust particles, straighten the flow, and reduce the freestream turbulence level, which is less than 1.5%.

The test section of the tunnel is 3-m long, 0.2–0.3-m high, and 0.3-m wide. This section consists of a flexible wall mechanism which is designed to provide a wide range of adverse pressure-gradient flows. The aspect ratios of lateral tunnel width to thermal and fluid boundary-layer heights was approximately 10 for most flow cases studied. The internal corners in the test section have 5-cm-radius fillets installed to reduce secondary flows. Additional sealing is achieved by taping the Plexiglas® doors to the test section from the sides.

The diffuser section is 2.26-m long and has an expansion area that provides a continuous transition from the rectangular cross-sectional area of the test section to a circular cross section of the fan. The converging and the diffuser sections are both attached to the test section. A thick rubber interface seal connects the diffuser section to the fan/motor drive system. The rubber internal seal acts as a shock absorber and prevents the fan vibration to be transferred to the main body of the wind tunnel.[9] The adverse pressure gradient wind tunnel is shown in Fig. 1.

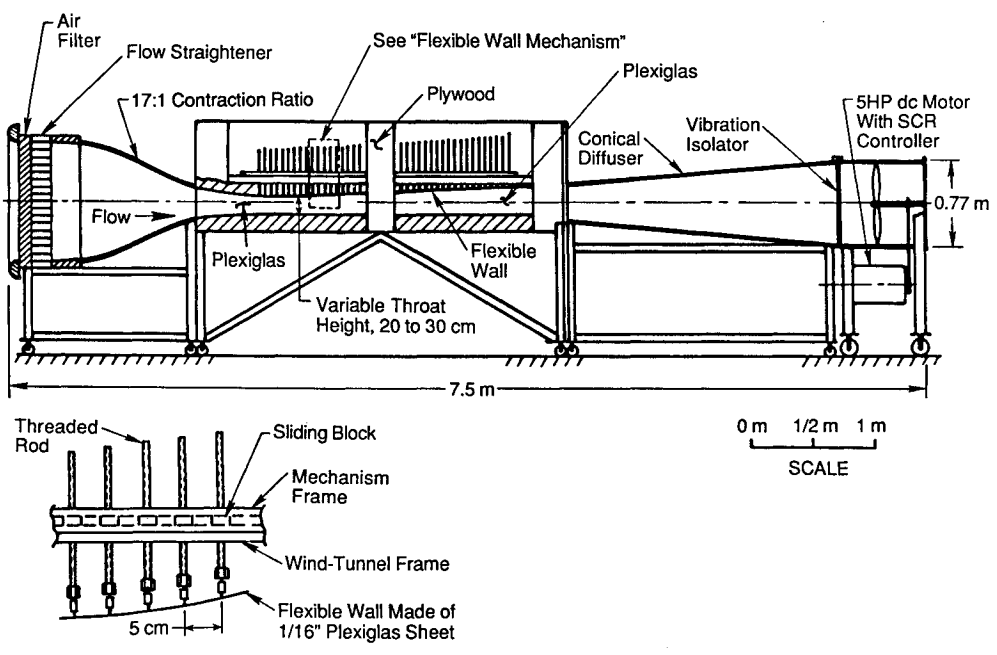

Fig. 1 Adverse-pressure-gradient wind tunnel.

Experimental Design

The flat plate consists of an unheated starting length and a heated portion, therefore, making the origins of momentum and thermal boundary layers different. The unheated starting length is 42.6 cm long with a leading-edge sandpaper surface 15.25 cm long for tripping the flow to insure the presence of a two-dimensional boundary layer.

The heated portion of the flat plate consists of 21 individually heated aluminium plates. The plates, which are 0.125-in. thick and come in two different sizes (10 by 1 in. or 10 by 6 in.), are installed in alternate fashion. The heated plates are separated from each other by 0.125-in.-thick cork board to minimize streamwise heat conduction, which also allows an accurate energy balance calculation to be made. The smaller-sized plates are used to provide an accurate measurement of the surface heat transfer rate as a function of downstream position. The plates are heated by custom manufactured silicon rubber heating elements. The power input to each plate is controlled by commercially available rhotostat switches.

The wall or surface temperature of the aluminium plates is measured using type E miniature thermocouples having a diameter of 0.127 mm. This type of thermocouple consists of Constantan-Chromel wires, and has the greatest sensitivity at room temperature. The wires are spot-welded at the junction.

Experimental Procedure and Measurement Techniques

Velocity Profiles

Mean and fluctuating components of the streamwise velocity profiles were measured using hot-wire anemometry. A Thermo System Inc. (TSI) anemometer, model 1050, with a frequency response of 100 kHz was used. The anemometer was operated in constant-temperature mode at an overheat ratio of 1.8. A TSI standard single-sensor boundary-layer probe, model 1218 T1.5, was used for both mean and fluctuating profile measurements. The sensor is a platinum-plated tungsten wire with a sensing diameter of 3.8 μ and a sensing length of 1.25 mm. The probe was connected to a DIGIMATIC traversing mechanism having a spatial resolution of 10 μ and traversed normal to the plate for the mean and fluctuating profiles. The anemometer signal was processed through a low-pass filter, Krohn-Hite model 3323, with a cutoff frequency which was determined after detailed analysis of the flow was made using Nicolet-660A digital spectrum analyzer. The signal was then measured with an IBM AT personal computer and IBM DACA board data-acquisition system.

Temperature Profiles

Mean and fluctuating temperatures were measured using a TSI model 1050 anemometer in constant current mode. The current was set at a value of 1.5 mA, as recommended by TSI, which resulted in a very low overheat. A TSI miniature standard single-sensor boundary-layer probe, model 1218 T1.5, was used for mean temperature profiles. A TSI subminiature straight probe, model 1276 P.5, was used for fluctuating temperature profiles. The sensor was a platinum wire with a sensing diameter of 1 μ and a sensing length of 1 mm. This sensor provides extremely high sensitivity to temperature fluctuations because of its small thermal inertia. A custom probe holder was designed and manufactured for the boundary-layer temperature measurements. The cutoff frequency was determined using the Nicolet power spectrum analyzer. The temperature probes were calibrated against a previously calibrated thermocouple in a uniformly heated stream. The detailed procedure for the cold-wire probes calibration for temperature measurements is given in Ref. 9.

Two-Point Correlations

Two-point correlation measurements were made for the temperature fluctuations. Two temperature probes were positioned for known longitudinal and normal distances between the two probes. For the normal correlation, one probe was held fixed at a reference y^+ value of about 35, and the other probe was traversed to different y^+ positions. For the longitudinal correlations, a single probe was held fixed at a given y^+ value, and the other probe was moved to different longitudinal (Δx^+) positions for the same y^+ value. The reference heights for the streamwise correlation were set at y^+ values of 75, 177, 270, and 420, which was the same range as the zero-pressure-gradient flow for later comparisons.

For the lateral movements, a special probe holder was designed and built to minimize flow disturbances. This probe holder has the capability of being moved laterally by sliding the holder in and out with respect to the test section, and at the same time registering the lateral movement with respect to a reference point. For this purpose a digital DIGIMATIC caliper, model 500-351, has been mounted on the holder to register the lateral movement with an accuracy of 10 μ.

A Cyborg ISAAC-2000 data-acquisition system in conjunction with an IBM/AT personal computer is used for two-point correlation measurements. The ISAAC-2000 has a maximum frequency response of 200 kHz with eight channels, with 624 K data-memory capabilities. The programming language "C" was used for data-acquisition triggering.

Presentation of Results

Two-Dimensional Fluid Dynamics

Spanwise uniformity of the flow at the measurement station was verified by measuring the velocity profiles at several spanwise positions with a hot-wire boundary-layer probe. The velocity defect profiles as a function of normal height were examined and it was felt there was reasonable agreement demonstrating the presence of a two-dimensional flow. Figure 2 shows the velocity defect profiles at five stations along the test section where an adverse-pressure-gradient flow exists. The normal height has been nondimensionalized with respect to the Clauser boundary-layer thickness. It is observed from the figure that an equilibrium adverse-pressure-gradient boundary layer is reached at a downstream distance from 87 to 137 cm, where the measured profile matches reasonably with the Clauser[10] profile for a β value of 1.8. On the same figure, the measured profile at the first station which has a zero-pressure-gradient matches the $\beta = 0$ profile.

Velocity Measurements

The universal mean velocity profiles nondimensionalized, with respect to the friction velocity, are shown in Fig. 3 for several positions along the adverse-pressure-gradient section of the tunnel's floor. The friction velocities were calculated using the Clauser technique. This technique was used for

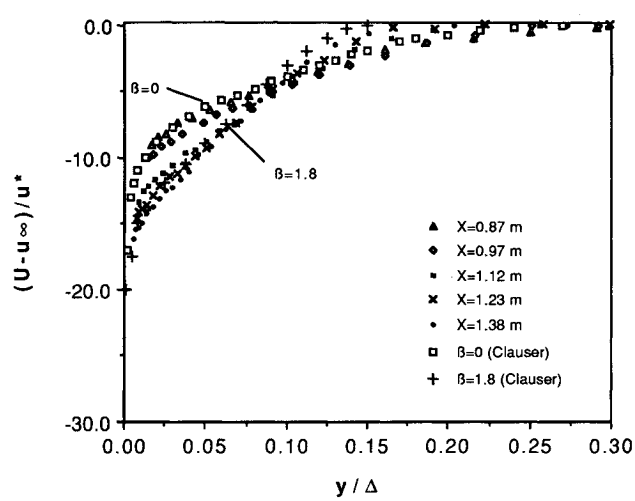

Fig. 2 Velocity defect profiles.

determination of the local skin-friction coefficient. The velocity data in the logarithmic core region fit the law-of-the-wall equation with constants given by Patel[11] as

$$u^+ = 5.5 \log y^+ + 5.45$$

The longitudinal velocity fluctuation measurements at the five stations are shown in Fig. 4. These fluctuations are higher than their corresponding zero-pressure-gradient fluctuations as presented in the first station profile, because of the decrease in the wall shear stress, or friction velocity. This effect is caused by the presence of the adverse-pressure-gradient. Table 1 lists the experimental parameters at the five stations within the adverse-pressure-gradient flow region of the test section.

Two-Dimensional Thermal Boundary Layer

The qualification of the two-dimensional thermal boundary layer was made by measuring the mean temperature profiles at measurement station 5 for three spanwise positions. The profiles, shown in Fig. 5, show reasonable agreement with each other. The temperature and the normal height have been nondimensionalized with respect to the temperature difference between the wall and the freestream values, and the thermal boundary-layer thickness, respectively.

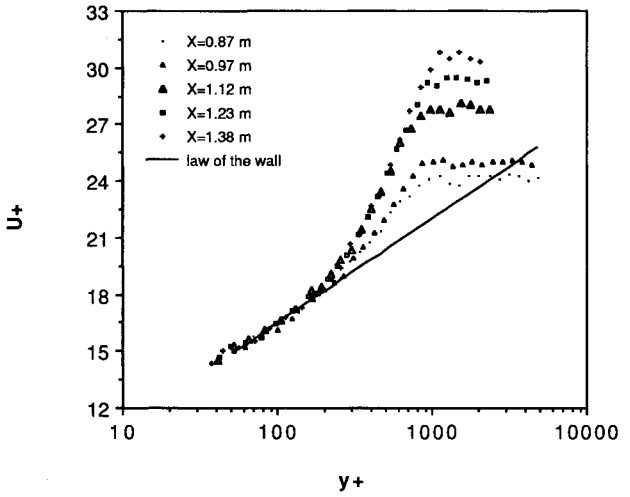

Fig. 3 Universal velocity law-of-the-wall, $\beta = 1.8$.

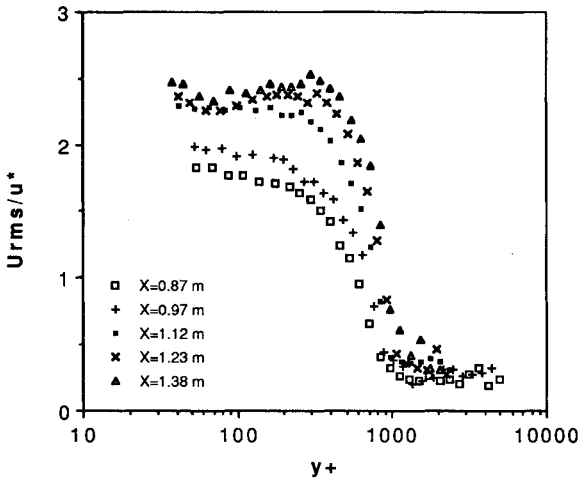

Fig. 4 Velocity fluctuation profiles.

Wall-Temperature Measurements

The uniformity of the wall temperature was checked by measuring the wall temperature along the heated portion of the plate. The measurements were made for each of the two temperature-difference cases along the centerline of the plate. The surface temperatures were measured with the thermocouples embedded in the heated aluminum plates, and show acceptable uniformity along the plate. For the 10 and 15°C temperature difference cases, the wall temperatures were uniform within ± 0.2, and ± 0.25°C, respectively.

Correlation Measurements

In this study, for the space-time correlation measurements, two temperature fluctuation probes were used to measure the temperature fluctuations simultaneously at two points in the spatial-temporal space. The two probes were positioned for known longitudinal and normal spatial distances between them. The turbulence signals from the two probes then were acquired and subsequently correlated.

The temperature cross-correlation coefficient is defined as

$$R_{T,T} = T(x, y, z, t)T(x + \Delta x, y + \Delta y, z + \Delta z, t + \Delta t)/[T_{\text{rms}}(x, y, z)T_{\text{rms}}(x + \Delta x, y + \Delta y, z + \Delta z)]$$

where T is the fluctuating temperature; T_{rms} is the root-mean-square value of T; (x, y, z) is the coordinate location of one probe in space; $(\Delta x, \Delta y, \Delta z)$ is the separation distance of the second probe from the first probe; t is the time coordinate; and Δt is the variable time shift. This cross-correlation coefficient is a measure of the similarity between the two temperature fluctuation signals. A high correlation between the

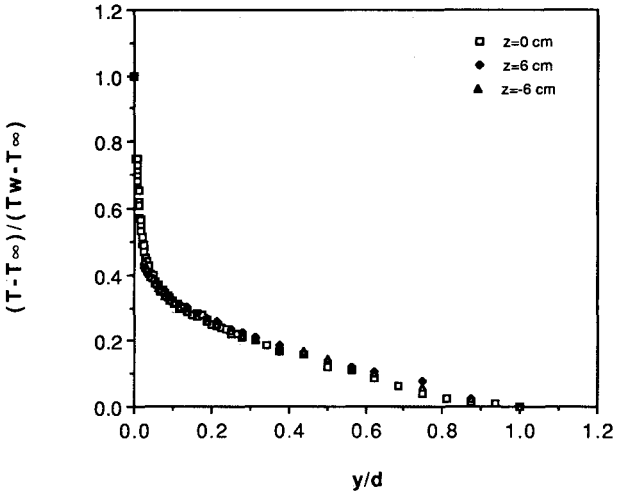

Fig. 5 Temperature profiles two-dimensionality check, $x = 1.38$ m.

Table 1 Values of experimental parameters

x, m	U, m/s	δ, cm	θ, cm	Re_θ	δ_t, cm $\Delta T = 10$°C	δ_t, cm $\Delta T = 15$°C	Δ, cm
0.87	17.8	1.94	0.190	2312	1.8	2.0	6.82
0.97	16.7	2.20	0.226	2494	2.1	2.3	7.90
1.12	15.4	2.40	0.300	3056	2.3	2.5	12.00
1.23	15.2	3.10	0.374	3810	2.7	3.0	16.10
1.38	14.5	3.26	0.444	4260	3.2	3.4	20.50

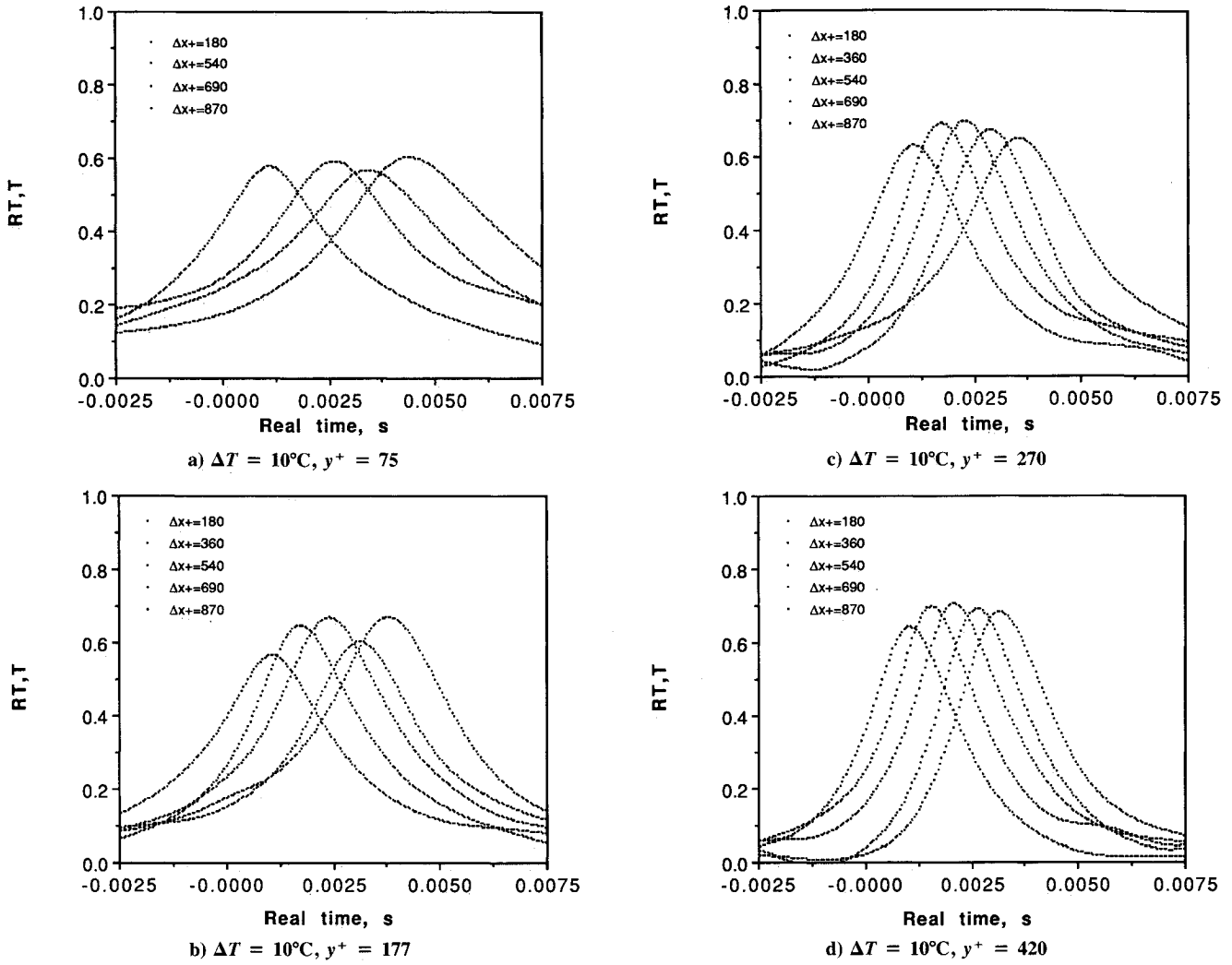

Fig. 6 Streamwise correlations.

two probes is an indication that the probes are monitoring the same or similar series of events including the passage of large-scale thermal structures, which in general, provide the highest degree of correlation. However, the correlation is less than unity as the events observed by the first will be altered due to the flowfield dynamics by the time they reach the second probe. The extent of similarity between the two signals depends on the absolute value of the cross-correlation coefficient. A high absolute value means that the two signals are highly correlated and are thought to be observing similar flow structure. The maximum absolute value of a correlation coefficient is equal to unity and only occurs when the correlation value of a signal being correlated with itself at the same time and is called autocorrelation. The autocorrelation coefficient can be calculated from cross-correlation coefficient when $\Delta x = \Delta y = \Delta z = 0$ for different times t.

Turbulent momentum and heat transport across a turbulent boundary layer are thought to be similar; however, the precise degree of similarity is not known. Since this transport of momentum and heat is associated with the turbulence structure near the wall, knowledge of the flow structure in this region of the flow is required. As mentioned before, this has been done in detail for isothermal zero-pressure-gradient flows. The same isothermal flow analysis for determining large-scale structure characteristics is now applied to a nonisothermal turbulent adverse-pressure-gradient boundary-layer flow.

Convection Velocity

The mean convection velocity of the temperature fluctuations was obtained from the correlation measurements in the streamwise direction ($\Delta y = \Delta z = 0$). Two temperature probes were positioned at different streamwise spacings and the same heights. The reference heights were set at y^+ values of 75, 177, 270, and 420 to obtain a distribution of the mean convection velocities of the T' structure. For each height and temperature difference case tested, five Δx^+ values were acquired. The space-time correlations of temperature fluctuations for the 10°C temperature difference value and the four reference heights are shown in Figs. 6a–d. Each figure con-

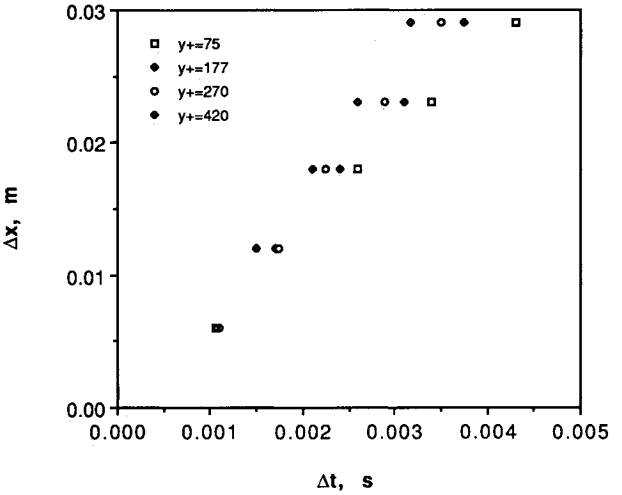

Fig. 7 Convection velocity determination, ΔT = 10°C.

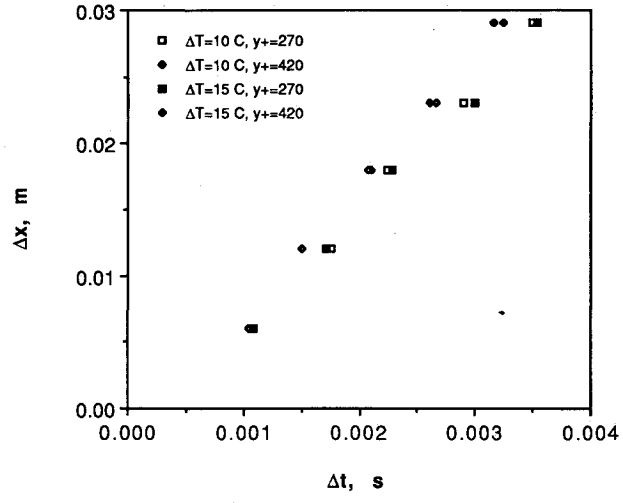

Fig. 8 Convection velocity determination, ΔT = 10 and 15°C.

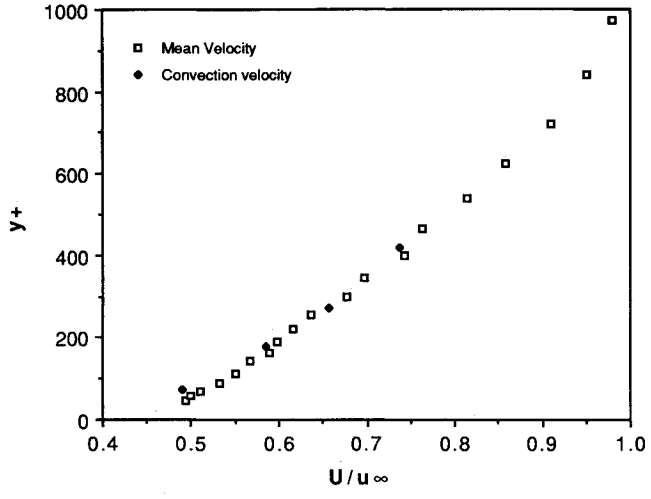

Fig. 9 Variation of the mean convection velocity, β = 1.8.

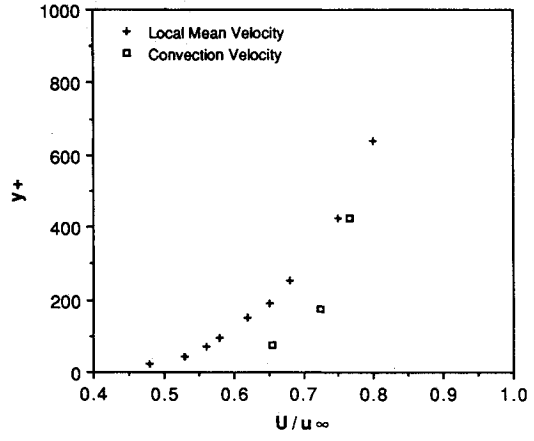

Fig. 10 Variation of the mean convection velocity, β = 0.

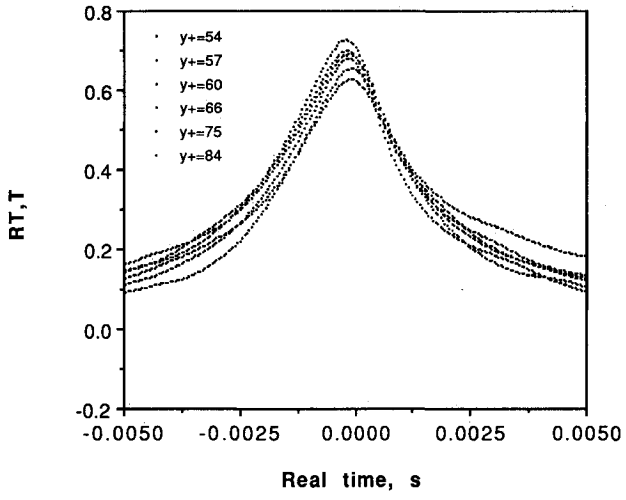

a) ΔT = 10°C

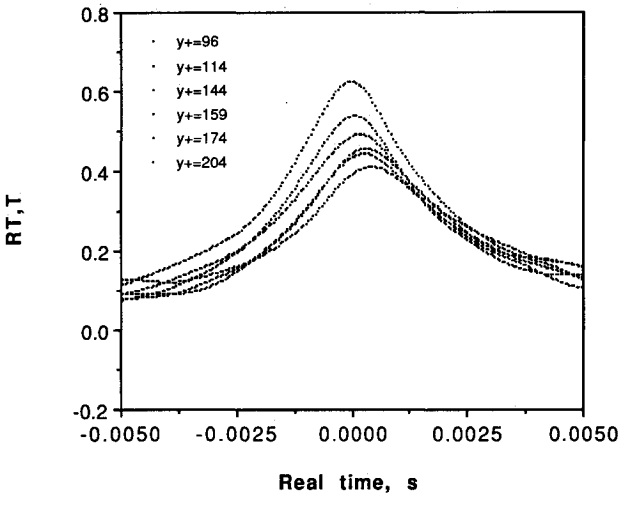

b) ΔT = 10°C

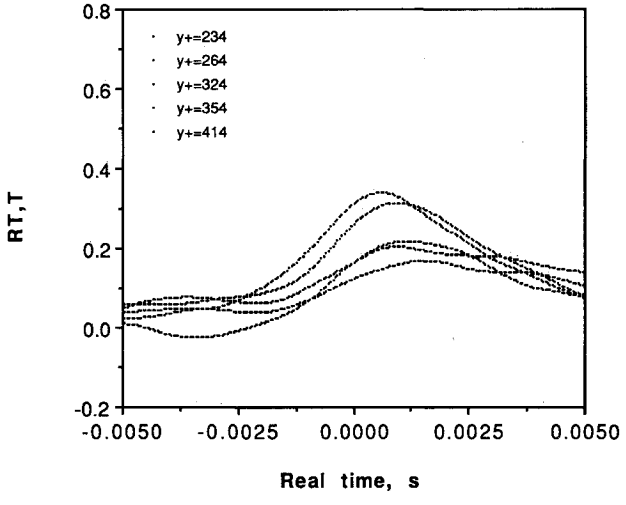

c) ΔT = 10°C

Fig. 11 Normal correlations at various heights.

tains the space-time correlations at the same height and different streamwise spacings between the probes.

From the space-time correlation measurements, the time shifts of the peak $R_{T,T}(\Delta x^+)$ from the zero time were measured. The time shifts, temporal displacements, are believed to be created by the passage of turbulent temperature fluctuation eddies which move with a convection velocity U_{cv}. The results of the spatial displacement vs the temporal displacement for the four reference heights are shown in Fig. 7 for the 10°C temperature-difference case. For the 15°C temperature difference, the results of the spatial displacement vs the temporal displacement for reference height values of y^+ equals 270 and 420 are shown in Fig. 8. On the same figure the corresponding 10°C results also are shown for comparison. The temporal displacements vary linearly with the streamwise separation and appear to be independent of the limited temperature differences tested. This result is consistent with the zero-pressure-gradient boundary-layer results.[9] The slope of each line in Figs. 7 and 8, $dx/dt = U_{cv}$, gives an estimate of

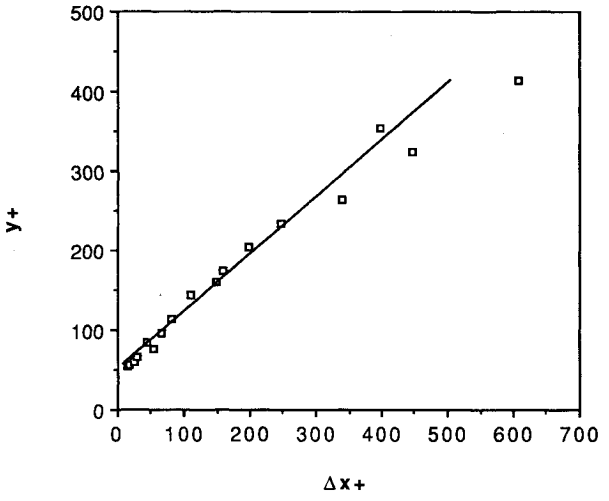

Fig. 12 Mean inclination angle of the T' structure.

the convection velocity of the temperature fluctuations at the given height.

Figure 9 displays the variation of the mean convection velocity with height described above. On the same figure the local mean velocity also is shown. The convection velocity of T' structure for the zero-pressure-gradient flow (Fig. 10) varied approximately from $0.65u_\infty$ at $y^+ = 75$ to $0.77u_\infty$ at $y^+ = 425$.[9] For the adverse-pressure-gradient case displayed in the figure, convection velocity varies from $0.48u_\infty$ at $y^+ = 75$ to $0.73u_\infty$ at $y^+ = 420$, which is approximately equal to the mean velocity profile. As seen from the figures, the convection velocity of the adverse-pressure-gradient flows is lower than the convection velocity of the zero-pressure-gradient case in the logarithmic core region of the boundary layer (i.e., y^+ less than 200–300). The effect of pressure gradient appears to have slowed the convection speed of the thermal structure, which suggests the effect of pressure gradient on the thermal structure is to slow the structure much quicker in the logarithmic core region unlike the zero-pressure-gradient case.

Inclination Angle

The mean inclination angle of the temperature fluctuations was obtained from the correlation measurements in the normal direction ($\Delta x = \Delta z = 0$). Two temperature probes were positioned at different normal spatial distances. One probe was held fixed at a reference height of $y^+ = 35$, while the other probe was traversed to different y^+ positions. The traversing probe was positioned at several points within the turbulent boundary layer.

From the space-time correlation measurements, the time shifts, temporal displacements, of the peak $R_{T,T}(\Delta y^+)$ correlation values from the zero time axis were measured. Figures 11a–c show some typical space-time correlations at different traversed probe heights. The values of the time shifts, along with the convection velocity $U_{cv}(y^+)$, were used to estimate the streamwise extent of the structure Δx^+ using Taylor's hypothesis, i.e.

$$\Delta x^+ = U_{cv}\Delta t u^*/\nu$$

The mean inclination angle is shown in Fig. 12. It is observed that the average inclination angle of the temperature fluctuation structure is about 32-deg inclined to the wall. This angle compares to an inclination angle of about 30 deg for the zero-pressure-gradient boundary-layer flows given in Bagheri and White.[8]

Conclusions

Space-time correlations of the temperature fluctuations, mean convection velocities, and the inclination angle of the large-scale structures were measured for an adverse-pressure-gradient turbulent boundary-layer flow over a heated surface with uniform wall temperature.

The mean convection velocity of the temperature fluctuation structures was determined to vary from $0.48u_\infty$ at $y^+ = 75$ to $0.73u_\infty$ at $y^+ = 420$, and appeared to be independent of the limited temperature-difference cases tested. The convection velocities were lower than corresponding convection velocity within the logarithmic core region of the zero-pressure-gradient case previously tested. The present convection velocities were found to be approximately equal to the mean local velocities.

The mean inclination angle of the temperature fluctuation structure was determined to be about 32 deg to the wall. The mean inclination angle was obtained from the correlation measurements in the normal direction. This inclination angle value agreed closely to the zero-pressure-gradient inclination angle of 30 deg. It is, however, believed that the inclination angle is a function of β, and further investigation should be carried out to find the precise dependency as a function of β.

References

[1]Kline, S. J., and Robinson, S. K., "Quasi-Coherent Structures in the Turbulent Boundary Layer: Part I. Status Report on a Community-Wide Summary of the Data," Zoran P. Zarić Memorial International Seminar on Near-Wall Turbulence, Dubrovnik, Yugoslavia, May 1988.

[2]Strataridakis, C. J., White, B. R., and Robinson, S. K., "Experimental Measurements of Large Scale Structures in an Incompressible Turbulent Boundary Layer Using Correlated X-Probes," AIAA Paper 89-0133, Jan. 1989.

[3]Kline, S. J., Reynolds, W. C., Schraub, F. A., and Runstadler, P. W., "The Structure of Turbulent Boundary Layers," *Journal of Fluid Mechanics*, Vol. 30, Pt. 4, 1967, pp. 741–773.

[4]Lian, Q. X., "Coherent Structures of Turbulent Boundary Layer in Flows with Adverse Pressure Gradient," Sino-U.S. Joint Fundamental Experimental Aerodynamics Symposium, Hampton, VA, June 1987.

[5]Smith, C. R., and Metzler, S. P., "The Characteristics of Low-Speed Streaks in the Near-Wall Region of a Turbulent Boundary Layer," *Journal of Fluid Mechanics*, Vol. 129, Pt. 1, 1983, pp. 27–46.

[6]White, J. B., and Tiederman, W. G., "The Effect of Adverse Pressure Gradient on Turbulent Burst Structure in Low-Reynolds Number Equilibrium Boundary Layers," Office of Naval Research, Rept. PME-FM-90-2, Jan. 1990.

[7]Bagheri, N., Strataridakis, C. J., and White, B. R., "Measurements of Turbulent Boundary Layer Prandtl Numbers and Space-Time Temperature Correlations," *AIAA Journal*, Vol. 30, No. 1, 1992, pp. 35–42.

[8]Bagheri, N., and White, B. R., "Experimental Measurements of Large Scale Temperature Fluctuation Structures in a Heated Incompressible Turbulent Boundary Layer," *International Journal of Heat and Mass Transfer* (to be published).

[9]Bagheri, N., "Turbulent Prandtl Number and Space-Time Temperature Correlation Measurements in an Incompressible Turbulent Boundary Layer," Ph.D. Dissertation, Univ. of California, Davis, CA, 1989.

[10]Clauser, F. H., "Turbulent Boundary Layers in Adverse Pressure Gradients," *Journal of Aeronautical Sciences*, Vol. 21, Feb. 1954, pp. 91–108.

[11]Patel, V. C., "Calibration of the Preston Tube and Limitations on Its Use in Pressure Gradients," *Journal of Fluid Mechanics*, Vol. 23, Pt. 1, 1965, pp. 185–208.